Elsevier Editorial System(tm) for Energy and Buildings
Manuscript Draft

Manuscript Number: ENB-D-11-00946R1

Title: Modelling a radiant floor system with Phase Change Material (PCM) integrated into a building simulation tool. Analysis of a case study of a floor heating system coupled to a heat pump.

Article Type: Full Length Article

Keywords: phase change material, thermal energy storage, floor heating, theoretical model

Corresponding Author: Mr. Javier Mazo,

Corresponding Author's Institution:

First Author: Javier Mazo

Order of Authors: Javier Mazo; Mónica Delgado; José María Marín, PhD; Belén Zalba, PhD

Abstract: This work describes a model developed to simulate a radiant floor system with PCM in simple building types. The building simulation model has been validated by comparing its behaviour with Energy Plus. The PCM radiant floor model is based on a one-dimensional finite difference scheme where the effective capacity method is used for PCM simulation. Some adjustments have been made to this one-dimensional scheme so that the thermal effect of two-dimensional heat transfer within the radiant floor slab is taken into account.
The results of an analyzed case study are also presented in this paper. Here, the PCM floor heating system is fed by a heat pump which mainly operates during night time, thus reducing the costs of electric energy consumption.

Title:

Modelling a radiant floor system with Phase Change Material (PCM) integrated into a building simulation tool. Analysis of a case study of a floor heating system coupled to a heat pump.

Authors:

Mazo Olarte, Javier (*); Delgado Gracia, Mónica; Marín Herrero, José María; Zalba Nonay, Belén

Aragón Institute for Engineering Research (I3A), Thermal Engineering and Energy Systems Group, University of Zaragoza.

Torres Quevedo Building, C/Maria de Luna 3, 50018 Zaragoza, Spain.

Phone: (+34) 976761000 ext: 5258, Fax: (+34) 976762616

* Corresponding Author, jmazo@unizar.es

Abstract

This work describes a model developed to simulate a radiant floor system with PCM in simple building types. The building simulation model has been validated by comparing its behaviour with Energy Plus. The PCM radiant floor model is based on a one-dimensional finite difference scheme where the effective capacity method is used for PCM simulation. Some adjustments have been made to this one-dimensional scheme so that the thermal effect of two-dimensional heat transfer within the radiant floor slab is taken into account.

The results of an analyzed case study are also presented in this paper. Here, the PCM floor heating system is fed by a heat pump which mainly operates during night time, thus reducing the costs of electric energy consumption.

Keywords: phase change material, thermal energy storage, floor heating, theoretical model.

Nomenclature

A	area [m^2]
ACH	air changes per hour [h^{-1}]
b	distance between tubes [m]
c_p	specific heat [J/(kg·K)]
d	pipe diameter [m]
e	window thickness [m]
F	view factor
G	irradiation [W/m^2]

h convection coefficient [W/(m^2·K)], enthalpy [kJ/kg]

I_d diffuse irradiation [W/m^2]

I_{dh} horizontal diffuse irradiation [W/m^2]

I_{dir} direct solar radiation [W/m^2]

J radiosity [W/m^2]

L length of pipe circuit [m]

$\dot{m}$ mass flow [kg/s]

n index of refraction

PCM Phase Change Material

$\dot{q}''$ heat flux per area unit [W/m^2]

$\dot{Q}$ thermal power, heat flux [W]

$R(\theta)$ reflectance

$R_{w\rightarrow slab}$ equivalent thermal resistance between water and concrete slab temperature [(m^2·K)/W]

T Temperature [ºC]

t time [s]

$T(\theta)$ transmittance

V volume [m^3]

$\dot{W}$ power consumption [W]

x cartesian coordinate [m]

Greek symbols

α spectral absorption coefficient [m^{-1}]

ε emissivity

λ thermal conductivity [W/(m·K)]

θ incidence angle [rad]

θ_{sun} solar elevation angle [rad]

ρ density [kg/m^3], reflectivity

σ Stefan-Boltzmann constant (σ=5.67·10^{-8} W/(m^2·K^4))

χ angle of refraction [rad]

Δx, Δt spatial and temporal increments

Subscripts

ext exterior

HP heat pump

LW long wave radiation

slab radiant floor slab

SW short wave radiation

w water, window

w,in inlet water

1. Introduction

Nowadays there is a need for more responsible energy use by developing more efficient systems, increasing the utilization of renewable energy resources and reducing fossil fuel consumption. Buildings constitute an important sector where improvements in energy use can be applied, since they account for nearly 40% of the final energy consumption in Europe. Phase Change Materials (hereafter PCM) can be used in buildings following different strategies. In passive applications, they can be incorporated into the building envelope and thus improve the thermal response of the building, reducing air heating or cooling requirements. Furthermore, they can be integrated into the storage devices of energy systems, allowing the use of renewable energy resources or improving the energy efficiency of those systems.

The present work is focused on the use of PCM in a radiant floor system. Radiant floor systems have the main advantage of working with lower temperature gradients compared to other conventional heating elements. Therefore, the energy efficiency of the equipment can be improved or low-grade energy sources can be used. Additionally, the incorporation of PCM provides an extra energy storage capacity that can be used for different purposes, such as levelling the energy demand or coupling the system to non time constant renewable energy sources. Despite the significant number of works in the literature dealing with the utilization of PCM in passive applications, not so many articles can be found on PCM in active building systems, such as ceiling panels or radiant floors. Lin et al. presented a numerical [1] and an experimental work [2] of an electric radiant floor system with shape stabilized PCM. In this case PCM was used to level the energy demand, as the heating energy consumption was made during the night producing savings in electric energy costs. Another example is the chilled ceiling panel with PCM developed by Koschenz and Lehmann [3]. This chilled ceiling panel device was designed to absorb a heat flux 40W/m^2 during 8 hours without producing an increase in temperature above the comfort range.

Ansuini et al. described in [4] the development and optimization of a radiant floor system with granulated PCM. In these three cases, PCM provides significant energy storage capacity and therefore the characteristic response time of these elements is considerably longer than that of traditional radiant systems. This characteristic makes these systems more suitable in applications where there is a significant delay between energy demand and supply.

Furthermore, Wang et al. [5] studied the performance of a cooling ceiling combined with a microencapsulated PCM slurry storage tank where chilled water was obtained by evaporative cooling technologies. Since a cooling ceiling panel works at relatively high temperatures (14-20ºC), it can use the cooling water generated by evaporative technologies [6]. The studied system produced an energy saving potential of up to 80% under climatic conditions in northwest China. Additionally, the use of PCM slurries as thermal storage material in cooling ceiling panels in order to shift the electric energy consumption of the chiller to night time was studied in [7].

The present work describes a model that has been developed in order to simulate a PCM radiant floor system in simple building types. The results of a case study are presented. In this application the PCM floor heating system is fed by a heat pump which operates mainly during night time. The radiant floor system is located in an experimental cubicle. In this case, the displacement of heating demand caused by the PCM involves appreciable savings in energy consumption costs.

2. Simulation

The simulation of radiant floor systems is necessary for the design of these applications and for the evaluation of their performance and technical feasibility. This simulation should be integrated within a building simulation program since the radiant floor interacts with other elements of the building (radiation heat exchange with other interior surfaces, convection heat transfer to the air, conduction heat transfer to other building elements).

The calculation of conduction heat transfer through PCM in building elements has special characteristics that involve some difficulties when integrating the calculation into a building energy simulation program. These special features are related to the non-linear behaviour of these materials within their phase change. Therefore the classical transfer function methods, widely used in calculating heat transfer through the building envelope, are not valid in the simulation of PCM. The most frequent solution to this problem is using a finite difference or finite volume scheme in order to calculate conduction heat transfer through building elements with PCM. These numerical algorithms should deal with the variation of the thermal properties of PCM during the phase change. Some building simulation programs allow the simulation of these materials; ESP-r [8] calculates heat transfer through the building envelope using a finite volume scheme, and PCM can be simulated using the special materials facility [9]. Energy Plus [10] incorporates a finite difference model that enables the calculation of PCM in the building envelope [11].

Although there are building simulation programs available that include models of PCM in the building envelope (passive applications), there are few models that allow the calculation of active building elements with PCM. This is due to the particular difficulties of the simulation of these systems, described in section 2.3 (multidimensional heat transfer in the element slab, control of the system). Energy Plus, for instance, did not include this active building element model until the version 6.0 (2010). The Energy Plus finite difference model for the simulation of active building elements is based on a one dimensional scheme so that it does not take into account the two dimensional effects of heat conduction. ESP-r also allows the simulation of active building systems with PCM but, as in the case of Energy Plus, this approach does not consider the multi dimensional conduction heat transfer in the slab since the Laouadi semi-analytical model [12] can not be used with PCM due to their non linear properties.

As a result, it was decided to develop a new model that enables the simulation of PCM in a radiant floor system. This is a simple building simulation model as it only permits the simulation of a single-zone building. It has been implemented using the equation solver program EES [13]. The main features of the model will be described in the following sections (sections 2.1 and 2.3).

2.1 Building model description

The building simulation model is based on a finite volume approach. It calculates heat transfer through the building envelope using a one dimensional finite difference model, and the zone calculation model uses a single node for the interior air temperature.

2.1.1 Heat transfer through the building envelope

Conduction heat transfer in the building envelope is calculated by a finite difference scheme. The heat transfer is assumed to be one dimensional and the thermal properties of the material are constant, except for the case of PCM. The numerical method uses an implicit method in order to avoid instabilities. A four node scheme is implemented for each building material layer.

2.1.2 Outside surface boundary conditions

Different modes of heat transfer are considered in the outside surface boundary condition. Each contribution is calculated separately. Figure 1 shows the different heat fluxes considered.

Radiation heat transfer

Radiation heat exchange between the outside surfaces of the building and the environment is calculated separately in two spectral ranges, short wave and long wave radiation.

Short wave radiation

Short wave radiation comprises direct solar radiation, diffuse solar radiation and solar radiation reflected from the ground (Eq. 1, 2). For the diffuse solar radiation, the anisotropic atmosphere model of Perez [14] has been implemented.

$$\dot{q}''_{SW,ext} = \dot{q}''_{directsolar} + \dot{q}''_{diffusesolar} + \dot{q}''_{groundreflected} \tag{1}$$

$$\dot{q}''_{SW,ext} = \varepsilon_{SW} \cdot \left(I_{dir} \cdot \cos(\theta) + I_d + F_{ground} \cdot \rho_{ground} \cdot \left[I_{dir} \cdot \cos(\theta_{sun}) + I_{dh} \right] \right) \tag{2}$$

where θ [radians] is the incidence angle of sun on the surface; I_d [W/m^2] is the surface incident diffuse radiation obtained from the anisotropic atmosphere model; I_{dir} [W/m^2] is the direct solar radiation; F_{ground} is the view factor of the outdoor surface to the ground; ρ_{ground} is the albedo; I_{dh} [W/m^2] is the horizontal diffuse radiation; and θ_{sun} [radians] is the sun elevation angle.

Long wave radiation

Outside building surfaces exchange heat with the ground, air and atmosphere [15] (Eq. 3).

$$\dot{q}''_{LW,ext} = \varepsilon_{LW} \cdot \sigma \cdot \left[\left(T_{ground}{}^4 - T_s{}^4 \right) \cdot F_{ground} + \left(T_{sky}{}^4 - T_s{}^4 \right) \cdot F_{sky} + \left(T_{air}{}^4 - T_s{}^4 \right) \cdot F_{air} \right] \tag{3}$$

The calculation of this heat flux has been linearized in order to simplify the numerical scheme. Thus, an equivalent heat transfer coefficient has been used. This coefficient is updated taking the previous time step surface temperature. This simplification has been assumed since the coefficient variation is small within the temperature range of the building surface.

Convection heat transfer

The convection coefficient is obtained from correlations. The correlations implemented in the model are the same as those used by Energy Plus in the ‘detailed’ algorithm [16]. The reason for the selection of these correlations is to simplify the validation process of the model, described in section 2.2, which has been carried out by comparing the simulation results with those obtained by Energy Plus.

2.1.3 Inside surfaces boundary conditions

As in the previous case, the three different modes of heat transfer are calculated individually. Figure 2 shows this heat balance graphically.

Radiation heat transfer: Short wave radiation

In this radiation exchange model, the following assumptions are made:

-Non participating medium.

-Grey surfaces.

-Direct solar radiation is uniformly reflected by inside surfaces.

This model needs the calculation of the incident direct solar radiation to the inside surfaces of the walls every time step, $I_{dir,i}$ [W/m^2]. This calculation is based on geometrical considerations.

The model is solved by the following linear system (Eq. 4, 5).

$$J_i - \sum_j \rho_{SW,i} \cdot F_{ij} \cdot J_j = \rho_{SW,i} \cdot I_{dir,i} \text{ , for an inside wall surface (i)} \tag{4}$$

$$J_w - \sum_j R_{d,w} \cdot F_{ij} \cdot J_j = T_{d,w} \cdot I_{d,w} \text{ , for the window inside surface} \tag{5}$$

where $R_{d,w}$ and $T_{d,w}$ are window reflectance and transmittance to diffuse solar radiation (section 2.1.4); and $I_{dir,i}$ [W/m^2] is the incident beam solar radiation to the surface i.

Therefore the heat transfer absorbed by each wall surface is (Eq. 6):

$$\dot{q}''_{SW,i} = \sum_j \rho_{SW,i} \cdot F_{ij} \cdot J_j + I_{dir,i} - J_i \tag{6}$$

Radiation heat transfer: Long wave radiation

The heat exchange between inside surfaces by long wave radiation is calculated by the network method proposed by Oppenheim [17]. The model considers uniform and grey surfaces in a non participating medium. In this model the glass of the windows is assumed to be opaque to long wave radiation. The radiation heat transfer is calculated from the following system of equations (Eq. 7):

$$\left(\sigma \cdot T_i^4 - J_i\right) \cdot \frac{A_i \cdot \varepsilon_{LW,i}}{1-\varepsilon_{LW,i}} - \sum_j \left(J_i - J_j\right) \cdot A_i \cdot F_{i,j} = 0 \tag{7}$$

The heat flux absorbed by each surface can be calculated using the following equation (Eq. 8):

$$\dot{q}''_{LW,i} = \left(J_i - \sigma \cdot T_i^4\right) \cdot \frac{\varepsilon_{LW,i}}{1-\varepsilon_{LW,i}} \tag{8}$$

The model has been linearized. Each time step and the equivalent heat transfer coefficient between each pair of surfaces are calculated using the previous time step surface temperatures.

Convection heat transfer

The convection heat transfer calculation algorithm is the same as that used for external surface calculations.

2.1.4 Window calculation

In the window calculation model, a single glass window is simulated. The input parameters that describe the behaviour of the glass are transmittance and reflectance to normal radiation (T(0) and R(0)). The window calculation model calculates the dependence of the incidence angle (θ) on transmittance and reflectance (Eq. 9, 10) [18].

$$T(\theta) = \frac{(1-\rho(\theta))^2 \cdot e^{-\alpha \cdot e / \cos\chi}}{1-\rho(\theta)^2 \cdot e^{-2 \cdot \alpha \cdot e / \cos\chi}} \tag{9}$$

$$R(\theta) = \rho(\theta)^2 \left(1 + T(\theta) \cdot e^{-\alpha \cdot e / \cos\chi}\right) \tag{10}$$

where e [m] is the glass thickness, and χ [rad] the angle of refraction, and α [m^{-1}] the spectral absorption coefficient.

In the glass reflectivity calculation, unpolarized radiation will be considered. Thus it can be expressed by equation 11 (Fresnel's equation).

$$\rho(\theta) = \frac{1}{2}\left(\left(\frac{n \cdot \cos\theta - \cos\chi}{n \cdot \cos\theta + \cos\chi}\right)^2 + \left(\frac{n \cdot \cos\chi - \cos\theta}{n \cdot \cos\chi + \cos\theta}\right)^2\right) \tag{11}$$

where n is the index of refraction.

For a given incident angle, the angle of refraction can be determined from the following equation (Eq. 12):

$$n \cdot \sin\chi = \sin\theta \tag{12}$$

Using the previous relationships, transmittance and reflectance are calculated for beam solar radiation and diffuse solar radiation.

The window heat balance is calculated by a finite difference scheme with two nodes per glass layer in which the heat capacity of the glazing material is neglected (Eq. 13, 14). Figure 3 shows the different heat fluxes included in the energy balance equation.

$$h_{convext} \cdot (T_{air} - T_{outglass}) + \dot{q}''_{LWext} + (T_{inglass} - T_{outglass}) \cdot \frac{\lambda_{glass}}{e} + \frac{\dot{q}''_{SWabsorved}}{2} = 0$$

$$h_{conv} \cdot (T_{air} - T_{inglass}) + \dot{q}''_{LW\,\mathrm{int}} + (T_{outglass} - T_{inglass}) \cdot \frac{\lambda_{glass}}{e} + \frac{\dot{q}''_{SWabsorved}}{2} = 0 \tag{13,14}$$

2.1.5 Interior air energy balance equation

It has been assumed that the temperature is uniform inside the cubicle, so that the stratification phenomena of indoor air are not considered in the model. Equation (15) is derived by an implicit method.

$$\rho_{air} \cdot c_{p,air} \cdot V_{air} \cdot \frac{T_{air,j} - T_{air,j-1}}{\Delta t} = \rho_{air} \cdot c_{p,air} \cdot V_{air} \cdot \frac{ACH}{3600} \cdot \left(T_{extair,j} - T_{air,j}\right) + \sum_{\text{int},surfaces} A_i \cdot h_{conv,i} \cdot \left(T_{s,i,j} - T_{air,j}\right)$$

(15)

2.1.6 Heat transfer through the ground

The model does not calculate conduction heat transfer in the ground. Therefore, an estimation of ground equivalent temperature has been made for the simulation.

2.2 Building model validation

The model validation has been made by comparing the results of the model with those given by Energy Plus. In these tests, the aim is to study the behaviour of the building simulation model, so that neither radiant floor operation nor PCM inclusion has been considered. Here the validation results of the experimental cubicle analyzed in the case study described in section 3 are shown. The dimensions of the cubicle and the thermo-physical properties of the materials are shown in figure 4 and table 1. The window is orientated to the north. No air infiltration is considered in the simulations presented here.

Two types of validation test have been performed: free floating interior temperature and ideal loads calculation. In the former, the interior temperature is not controlled. Temperatures of the interior air and all the building surfaces have been compared. In the latter, ideal thermal loads are calculated. The comparison between both models has been done in different periods of the year.

The validation results are quite good, the difference in temperature calculation being less than 0.3ºC and in the ideal thermal loads calculation less than 1%. Figure 5 shows the interior air temperature calculated with both models in the free floating temperature simulation. In figure 6, the calculated thermal loads can be compared.

2.3 Modelling of a radiant floor with PCM

The simulation of radiant floor systems is relatively complex, as different heat transfer processes are involved: heat conduction in the floor slab, heat radiation exchange between the floor surface and other internal surfaces, heat transfer in the floor piping. Since there is no analytical solution for these heat transfer problems, finite difference or finite element methods should be used to calculate heat transfer in the radiant floor slab. This approach has been used by several authors using two-dimensional numerical schemes to analyse these systems [19]. The problem with such methods is the high computational effort involved. In order to integrate these models into building simulation programs, simpler numerical models have been developed by different authors. Several approaches have been used in the simulation of these active systems: conduction transfer function models, semi-analytical models, and thermal resistance and capacitance network models (hereafter RC models).

Strand [20] developed a transfer function-based model for thermally activated system simulation. The conventional transfer function method was modified in order to include a source term which models heat transfer between the tubes and the concrete slab. As has been mentioned, this method can not be used in PCM simulation because of the non linear behaviour of the material.

Laouadi [12] conducted a semi-analytical study in order to obtain a radiant floor model. By using this method, an analytical expression was obtained to correct the calculation of the one dimensional model integrated in ESP-r. This method was based on the linear properties of building material so that, being rigorous, it is not valid for PCM simulation.

The aim of RC models is to obtain a thermal network, composed of resistances and capacitances, in order to simulate heat transfer in the activated building component. This thermal network enables the dynamical performance of active building systems to be calculated with a low consumption of CPU time.

Koschenz and Dorer [21] developed a radiant element model where heat transfer between the tubes and the slab was modelled by a resistance link. Heat transfer within the slab was calculated by a one dimensional scheme. The resistance link was calculated from the stationary solution, using form factors. This model was implemented in TRNSYS [22], where the resistance link was coupled to the conduction transfer function method used by the program. Ren et al [23] also used a parameter estimation of the RC network based on geometrical considerations in the modelling of a ventilated concrete slab.

Another approach to this parameter estimation is the optimization of those values using the thermal response to sinusoidal excitation. This methodology is based on the work of Akander [24], who optimized the dynamical response of these models using the frequency domain analysis. Weber et. al [25, 26] obtained optimised RC models and studied the optimisation of different RC configurations. The thermal response of the RC model was compared to a two-dimensional finite element model working in the frequency domain.

Although this last approach is the most suitable for integrating a radiant floor model into a building simulation program, since it simulates quite accurately the behaviour of a radiant system with low computational effort, it is not possible to use it with PCM; frequency domain analysis can not be used for radiant floor with PCM due to their non-linear properties.

2.3.1 Radiant floor model

When simulating PCM in radiant elements, only finite difference or finite element methods can be utilised. Furthermore, two-dimensional conduction heat transfer effects should be accounted for. Laouadi remarks in his work [12] that one-dimensional models under-predict the circuit water temperature, involving an over-prediction of the heating/cooling capacity of the boiler/chiller.

The solution adopted in the present work is implementing a modified one-dimensional model that considers these two-dimensional effects. A similar idea was used by Koschenz and Dorer [21]. Thermal resistance that links the pipe water temperature and the concrete slab temperature ($R_{w\rightarrow slab}$, in fig. 7) is modified so that the calculated heat flux in stationary conditions is the same using both schemes (one and two-dimensional method). The resulting one-dimensional scheme can be represented as the thermal network shown in figure 7. The number of temperature nodes in the figure has been reduced in order to clarify the picture.

This simplification of the two-dimensional heat transfer has been tested by analysing the thermal dynamical response. The one-dimensional model has been compared to a two-dimensional one. In order to evaluate the performance of the simplified model, two characteristic transient processes have been defined: *charge* and *discharge processes*. In the *charge process* the concrete slab will be initially in thermal equilibrium with the ambient air and then the water begins to flow through the pipes at a constant temperature. In the *discharge process* the system originates with a stationary situation when the water flow stops. In both cases it will be considered that the lower surface is thermally isolated. An example of the performance of these two models is shown in figure 8, where the floor surface heat flux during the two transient processes is plotted. The geometrical data and thermo-physical properties of the materials are shown in tables 2 and 3. The boundary conditions are shown in table 2. In this case the simulated radiant floor contains 20% of PCM in the concrete slab.

The thermal response of both models is very similar. The difference in the heat flux in the floor surface is less than 10% between the two models, and the reaction time of both models is nearly the same.

2.3.2 Heat transfer in radiant floor piping

In the heat transfer model between the floor piping and the concrete slab, certain assumptions have been made:

-The radiant floor temperature along the water circuit is considered uniform.

-Thermal inertia of the water will be neglected.

This heat transfer model is based on the same assumptions as that implemented in Energy Plus [16, 20]. The resulting heat balance differential equation for the water flux through the pipe is shown below (Eq. 16,17).

$$\dot{m}_w \cdot c_{p,w} \cdot \frac{\partial T_w(x)}{\partial x} = -\frac{\pi \cdot d}{R_{w\rightarrow slab}} \cdot \left(T_w(x) - T_{slab}\right) \tag{16}$$

$$T_w(x=0) = T_{in,w} \tag{17}$$

where $R_{w\rightarrow slab}$ [(m^2·K)/W] is the equivalent heat transfer resistance between water and the concrete slab temperature that includes the two-dimensional effects of heat transfer. Solving the previous differential equation (Eq. 16-17), the boundary condition that will be used in the one-dimensional conduction heat transfer model is obtained (Eq. 18).

$$\dot{q}''_{w\rightarrow slab} = \frac{\dot{m}_w \cdot c_{p,w}}{L \cdot b} \cdot \left(T_{in,w} - T_{slab}\right) \cdot \left(1 - e^{-\frac{\pi \cdot d \cdot L}{\dot{m}_w \cdot c_{p,w} \cdot R_{w\rightarrow slab}}}\right) \tag{18}$$

2.3.3 PCM modelling

Heat transfer in PCM building materials is calculated using the effective capacity method, which is based on the enthalpy method. Both formulations are frequently used in heat transfer calculations in PCM for building applications. The main advantage of these methods is that a single formulation is valid for the entire problem domain and there is no need to track the phase change boundary [27].

The heat capacity method uses a temperature-dependent heat capacity rather than the enthalpy-temperature function in order to calculate the energy time variation. There are several examples in the literature of using this approach [3, 28-30].

The assumptions that have been made in the model are:

-The composite PCM material will be analyzed as a uniform material with homogeneous equivalent properties. This assumption is commonly considered in building energy simulation with PCM [3, 28-30].

-The heat transfer is one-dimensional: as has been described (section 2.3.1), conduction heat transfer in the radiant floor slab can be simplified to a one-dimensional scheme.

-All the thermo-physical properties, except heat capacity, will be considered constant. Considering temperature variation in these properties would involve very accurate measurements but the influence of this variation may not be significant in the simulation results.

The one-dimensional heat transfer equation utilised is shown below (Eq. 19).

$$\rho \cdot c_p(T) \cdot \frac{\partial T}{\partial t} = \lambda \cdot \frac{\partial^2 T}{\partial x^2} \qquad (19)$$

An analytic expression for heat capacity variation with temperature is needed. This expression has been fitted from experimental measurements (section 3.1.2).

The equation is discretized using a finite difference scheme. Time variation is evaluated with an implicit formulation in order to avoid instabilities. However, thermal heat capacity is evaluated with the previous time step temperature (Eq. 20). Hence the solution algorithm of the numerical scheme is simpler as it can be solved in each time step using a linear system of equations. A similar approach was used by Kuznik et al. [29].

$$\rho \cdot c_p\left(T_i^{\,j-1}\right) \cdot \frac{T_i^{\,j} - T_i^{\,j-1}}{\Delta t} = \lambda \cdot \frac{T_{i+1}^{\;\;j} - 2 \cdot T_i^{\,j} + T_{i-1}^{\;\;j}}{\Delta x^2} \qquad (20)$$

3. Analysis of a case study

The developed model described in the previous sections has been utilised to analyse the performance of a radiant floor system with PCM in a particular application. In this case study, the floor heating system obtains the hot water supply from a heat pump. Thermal energy storage is used to move electric energy consumption from daytime to night time. This strategy can reduce energy costs as most of the energy consumption is produced during off-peak hours.

3.1 Description

3.1.1 Experimental cubicles

The experimental cubicles used in this analysis are the same as those defined in section 2.2, on validation of the developed model. These cubicles are located in Córdoba (Spain) and the weather data is extracted from the Energy Plus weather data base [10].

3.1.2 Concrete with PCM compound in radiant floor slab.

The PCM is integrated into the radiant floor by being embedded in the concrete material of the slab. The simulated PCM is a granulated compound material. The phase change temperature is near 27ºC. In the following figure the enthalpy-temperature curve of this material is shown (fig. 9). This curve has been obtained using the T-history method [31].

The geometrical parameters and material properties have been defined in section 2.3.1. The amount of PCM included in the radiant floor has been adjusted to achieve the total shift of the heating energy demand from peak hours to off-peak hours. The obtained quantity of PCM is a 20% proportion in mass in the mortar-PCM composite.

3.1.3 Heat pump modelling

The heat pump modelling is based on correlations provided by CIAT. The heat pump modelled is a commercial air to water heat pump.

The correlations calculate the maximum heating or cooling power, as well as the electric power consumed, for given conditions of air temperature (T_{air}) and water temperature (T_{water}). Both electric power consumption ($\dot{W}_{HP}$) and supplied heating power ($\dot{Q}_{HP}$) are correlated by a quadratic expression (Eq. 21). When the machine operates at partial load, a factor is used to correct the coefficient of performance.

$$\dot{W}_{HP} = a + b \cdot T_w + c \cdot T_{air} + d \cdot T_w{}^2 + e \cdot T_{air}{}^2 + f \cdot T_w \cdot T_{air} \quad (21)$$

3.1.4 System control

The water supply temperature set point is fixed at a constant temperature of 33ºC. With this temperature level the heating demand can be met and the on-off switches are reduced. The control of the system utilized is simple: an on-off control with an interior air set point temperature of 21ºC.

3.1.5 Electric energy pricing

As the analysis includes a calculation of the savings in electric energy cost, an electrical energy market framework has to be selected. In this case the Spanish legislation has been chosen. According to this, off-peak demand time is from 22h to 12h. The energy price during peak load hours is 0.169€/(kW·h) and during valley load hours 0.061€/(kW·h). The electric energy price with no differentiation between peak and off-peak hours is 0.14€/(kW·h).

3.2 Simulation results

Two case studies have been done, one with PCM and the other with a conventional radiant floor system, in order to make a comparison of the results.

3.2.1 Analysis of the results: a characteristic winter day performance

First of all, the performance of the system during a characteristic winter day will be analysed. The influence of the PCM in the radiant floor is quite remarkable. In figure 10, the performance of the system is characterized by the interior air temperature fluctuation and energy consumption of the heat pump. The electric energy power consumed by the machine has been rated per square metre of the experimental cubicle floor surface.

Some important features of the performance of the PCM radiant floor systems should be highlighted:

-Due to the additional energy storage of the PCM, the whole energy consumption can be moved to off-peak hours of electric energy demand.

-The operation of the heat pump is more uniform, and there are fewer stops in its performance. This effect is due to the higher thermal inertia of the PCM radiant floor.

-The cubicle with PCM presents a wider temperature fluctuation. In the midday hours, when no heating is needed, the temperature in the PCM cubicles rises to 25 ºC. This temperature increase is due to the extra thermal energy storage provided by the PCM. This has to be allowed in order to ensure comfort temperature conditions in the evening (20-22h) without the operation of the heat pump.

3.2.1 Simulation of both systems during a winter season

The simulation of both cubicles during a whole winter period has been carried out in order to obtain average values of their performances and of the cost energy savings produced by the PCM. The simulation period was selected according to the heating energy demand, starting on November 1st and finishing on February 28th. Some important values of the performance of both systems are shown in table 4. In the following figure (fig. 11) the interior air temperature fluctuation of both cubicles is plotted. It can be seen that both systems are able to meet each cubicle heating requirement as the interior air temperature during most of the time is within the comfort range of 20-25ºC.

Some conclusions can be obtained from these simulations:

-The energy consumption of both cubicles is very similar. In this case, the addition of PCM does not produce energy savings.

-The energy cost savings are only due to the energy consumption displacement to the off-peak electricity demand period.

4. Conclusions

A new model has been developed in order to simulate a radiant floor system with PCM integrated into a building energy simulation tool. The developed model enables the simulation of simple buildings, with just one zone, which can include active elements with PCM. The validation has been done by comparing its results with Energy Plus. In this comparison neither active systems nor PCM are included. The validation tests have been satisfactory: the difference in temperature evolution was less than 0.3ºC and in the ideal loads calculation less than 1%. A modified one-dimensional model was selected to simulate the radiant floor behaviour. The thermal response of this model was compared to a more realistic two-dimensional model with reasonably acceptable results. The response times were quite similar and the error in the surface heat transfer calculation was less than 10%.

A case study has been analysed using the previously described model. In this application a floor heating system is fed by a heat pump. The PCM is used in order to provide the radiant system with enough storage capacity to avoid the operation of the heating pump during the peak electricity demand period. As has been seen, the radiant floor with PCM is able to meet the heating demand requirements with a practically total shift of the electric energy consumption from the peak period to the off-peak electricity demand time. This effect implies an energy consumption cost saving of nearly 18% compared to the conventional case.

This case study has been interesting from the point of view of the results obtained by the developed model and also for demonstrating the technological feasibility of the floor heating system analyzed. However, there are some features of the simulations that should be remarked on and taken into consideration when extracting general conclusions about the performance of these PCM radiant floor systems. First of all, the thermal behaviour of the experimental cubicles where the simulated radiant floors were studied is quite different from a conventional building thermal response. It would be interesting in subsequent studies to analyze the operation of this new system in traditional buildings. In addition, the experimental cubicles were located in a mild winter weather zone, where the required heating energy consumption is low. In the future, economic feasibility studies should be orientated to cases where the winter weather is colder and where a more profitable use of the PCM can be obtained.

5. Acknowledgements

The authors would like to thank the Spanish government for the partial funding of this work within the framework of the research project ENE2008-06687-CO2/CON (MICINN-FEDER). The authors would also like to thank the CIAT company for its participation and support within the framework of the SOLTES project, partially funded by the Innovation and Development Agency of Andalucía (IDEA) and CDTI (Industrial Technological Development Centre). Javier Mazo is especially grateful to the government of Aragón for a grant.

Bibliography

[1] K. Lin, Y. Zhang, X. Xu, H. Di, R. Yang, Penghua Qin, Modeling and simulation of under-floor electric heating system with shape-stabilized PCM plates, Building and Environment 39 (2004) 1427-1434.

[2] K. Lin, Y. Zhang, X. Xu, H. Di, R. Yang, P. Qin, Experimental study of under-floor electric heating system with shape-stabilized PCM plates, Energy and Buildings 37 (2005) 215-220.

[3] M. Koschenz, B. Lehmann, Development of a thermally activated ceiling panel with PCM for application in lightweight and retrofitted buildings, Energy and Buildings 36 (2004) 567-578.

[4] R. Ansuini, R. Larghetti, A. Giretti, M. Lemma, Radiant floors integrated with PCM for indoor temperature control, Energy and Buildings 43 (2011) 3019-3026.

[5] X. Wang, J. Niu, A.H.C. van Paassen, Raising evaporative cooling potentials using combined cooled ceiling and MPCM slurry storage, Energy and Buildings 40 (2008) 1691-1698.

[6] J. Niu, J.v.d. Kooi, H.v.d. Rhee, Energy saving possibilities with cooled-ceiling systems, Energy and Buildings, Volume 23 (1995) 147-158.

[7] X. Wang, J. Niu, Performance of cooled-ceiling operating with MPCM slurry, Energy Conversion and Management, 50, (2009) 583-591.

[8] ESRU, ESP-r, http://www.esru.strath.ac.uk/Programs/ESP-r.htm, access date: November 2th, 2011.

[9] D. Heim, J.A. Clarke, Numerical modelling and thermal simulation of PCM–gypsum composites with ESP-r. Energy and Buildings 36 (2004) 795-805

[10] EnergyPlus. http://www.eere.energy.gov/buildings/energyplus/, access date: November 2th, 2011.

[11] C.O. Pedersen, Advanced zone simulation in EnergyPlus: Incorporation of variable properties and Phase Change Material (PCM) capability, Proceedings: Building Simulation (2007).

[12] A. Laouadi, Development of a radiant heating and cooling model for building energy simulation software, Building and Environment 39 (2004) 421-431.

[13] S. A. Klein, Engineering equation solver (EES), F-Chart Software & McGraw-Hill (2003).

[14] R. Pérez, P. Ineichen, R. Seals, J. Michalsky and R. Stewart, Modeling daylight availability and irradiance components from direct and global irradiance, Solar Energy 44 (1990) 271-289.

[15] T. M. McClellan, and C. O. Pedersen, Investigation of Outside Heat Balance Models for Use in a Heat Balance Cooling Load Calculation. ASHRAE Transactions, Vol. 103, Part 2 (1997) 469-484.

[16] The Reference to EnergyPlus Calculations. Energy Plus Engineering Reference.

[17] A. K. Oppenheim, Radiation Analysis by the Network method, Transactions of the ASME, vol. 78 (1956) 725-735.

[18] R. Siegel, J.R. Howell, Thermal Radiation Heat Transfer, 2nd edition, Hemisphere Publishing Co., 1981.

[19] K. Fort, Type 160: floor heating and hypocaust, Transsolar Energietechnik GmbH, Stuttgart, Germany (1999).

[20] R.K. Strand, K.T. Baumgartner, Modeling radiant heating and cooling systems: integration with a whole-building simulation program, Energy and Buildings 37 (2005) 389-397.

[21] M. Koschenz, V. Dorer, Interaction of an air system with concrete core conditioning, Energy and Buildings 30 (1999) 139-145.

[22] S.A. Klein, W.A. Beckman and J.W. Mitchell et al., TRNSYS, a Transient Simulation Program: Version 16.1, University of Wisconsin, Solar Energy Laboratory, USA (2006).

[23] M.J. Ren and J.A. Wright, A ventilated slab thermal storage system model, Building and Environment 33 (1998) 43–52.

[24] J. Akander, The ORC method effective modelling of multilayer building components. Doctoral Dissertation Division of Building Technology, Department of Building Sciences KTH-Royal Institute of Technology Stockholm, Sweden, 2000.

[25] T. Weber, G. Jóhannesson, An optimized RC-network for thermally activated building components, Building and Environment 40 (2005) 1-14

[26] T. Weber, G. Jóhannesson, M. Koschenz, B. Lehmann, T. Baumgartner, Validation of a FEM-program (frequency-domain) and a simplified RC-model (time-domain) for thermally activated building component systems (TABS) using measurement data, Energy and Buildings 37 (2005) 707-724.

[27] B. Zalba, J.M. Marín, L. Cabeza and H. Mehling, Review on thermal energy storage with phase change: materials, heat transfer analysis and applications, Applied Thermal Engineering 23 (2003) 251–283.

[28] K. Darkwa and P. O'Callaghan, Simulation of phase change drywalls in a passive solar building, Applied Thermal Engineering 26 (2006) 853–858.

[29] F. Kuznik, J. Virgone and K. Johannes, Development and validation of a new TRNSYS type for the simulation of external building walls containing PCM, Energy and Buildings 42 (2010) 1004–1009.

[30] M. Zukowski, Mathematical modeling and numerical simulation of a short term thermal energy storage system using phase change material for heating applications, Energy Conversion and Management 48 (2007) 155–165.

[31] J.M. Marín, B. Zalba, L.F. Cabeza, H. Mehling, Determination of enthalpy-temperature curves of Phase Change Materials with the T-history method – Improvement to temperature dependent properties, Energy and Buildings 37 (2005) 215-220.

Table(s) with Caption(s)

Walls	Thickness [mm]	λ [W/(m·K)]	ρ [kg/m^3]	c_p [J/(kg·K)]
Sandwich panel (PU)	40	0.0184	40	1760
Roof	Thickness [mm]	λ [W/(m·K)]	ρ [kg/m^3]	c_p [J/(kg·K)]
Roof cover	0.6	50	7800	560
Fiber glass	80	0.04	12	870
Roof cover	0.6	50	7800	560
Floor	Thickness [mm]	λ [W/(m·K)]	ρ [kg/m^3]	c_p [J/(kg·K)]
Isolating material (PU)	40	0.0184	40	1760
Mortar	60	1,4	2100	850
Floor tile	12	2	2000	1500

Table 1. Thermal properties of the materials.

Distance between pipes	120 mm	Ambient air temperature	20ºC
Pipe diameter	20 mm	Water temperature	32ºC
Mortar layer thickness	60 mm	Heat transfer coefficient at floor surface	7 W/(m^2·K)
Floor tile thickness	12 mm		

Table 2. Geometric parameters of the radiant floor and boundary conditions.

Mortar	ρ [kg/m³]	cp [kJ/(kg·K)]	λ [W/(m·K)]
	2100	850	1.4
Floor tile	ρ [kg/m³]	cp [kJ/(kg·K)]	λ [W/(m·K)]
	2000	1500	2

Table 3. Thermal properties of radiant floor materials.

	with PCM	**without PCM**
Mean daily energy consumption	2.62 (kW·h)/cubicle	2.60 (kW·h)/cubicle
Daily operating time	7.5 h/day	7.7 h/day
Daily operating time in peak period	0.3 h/day	1.4 h/day
Mean daily costs	0.17€/day	0.21€/day
Cost savings	17.9%	-

Table 4. Results of the simulations.

List of Figure Captions

Figure(s)
[Click here to download high resolution image]

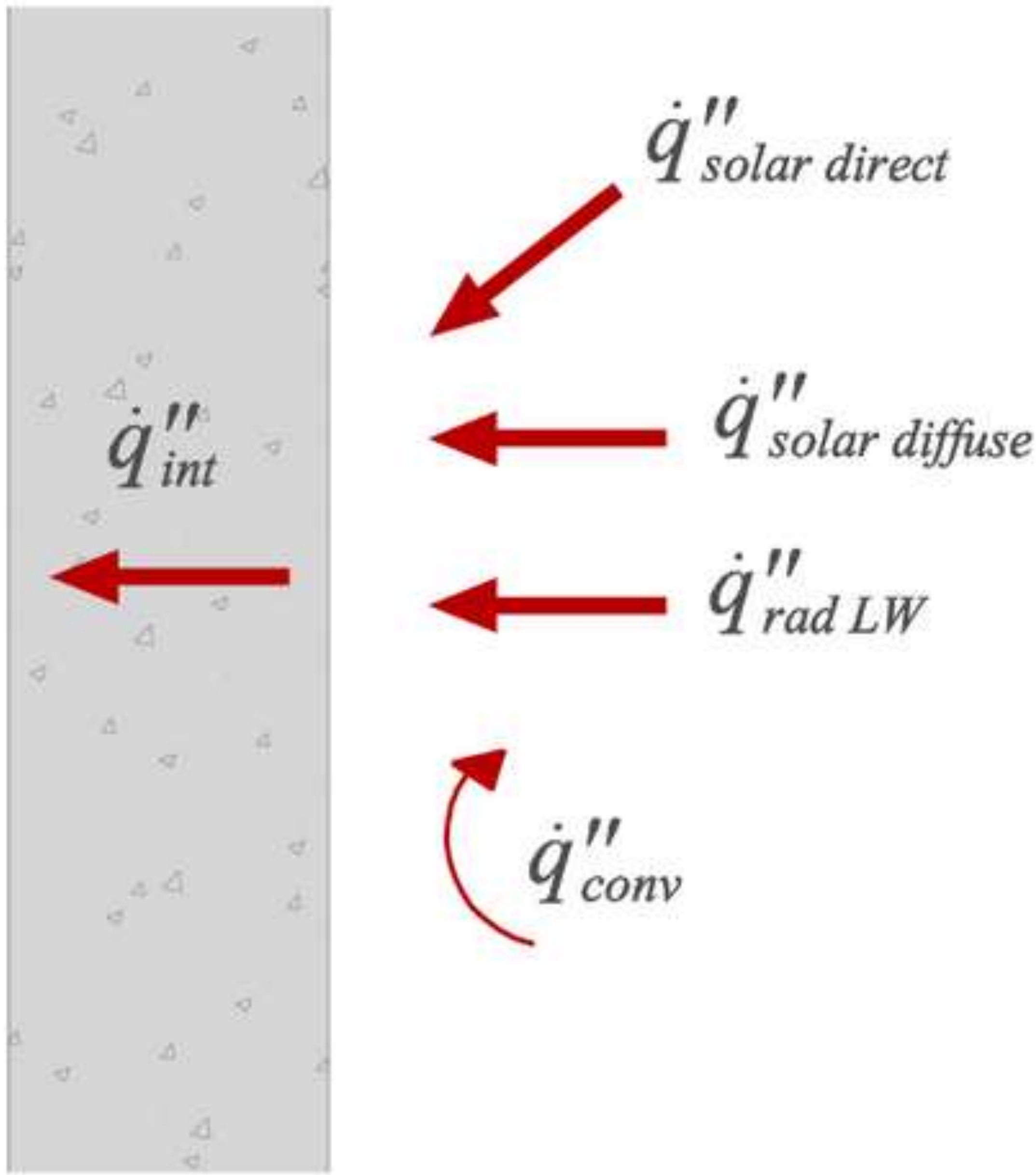

Figure(s)
Click here to download high resolution image

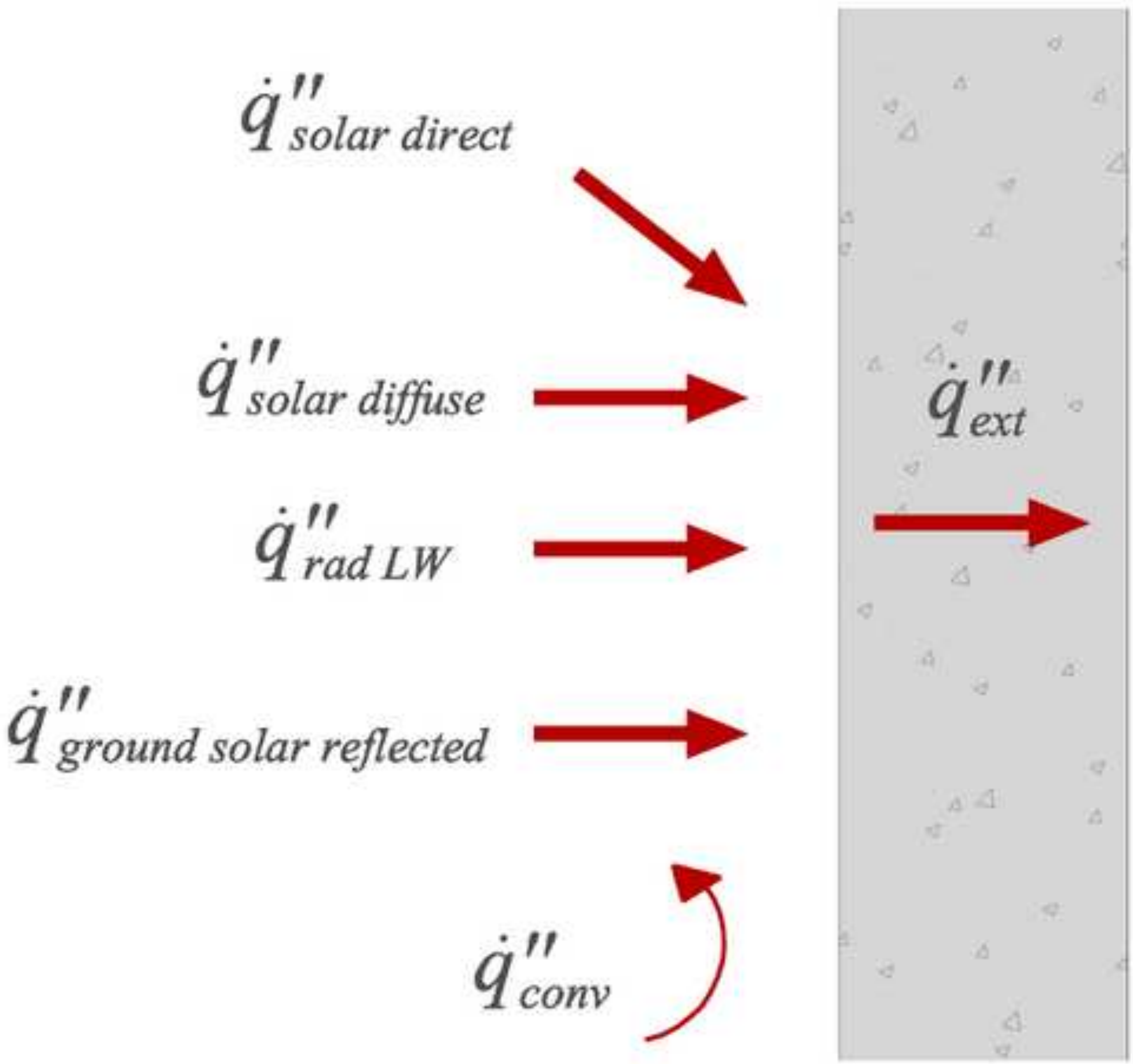

Figure(s)
Click here to download high resolution image

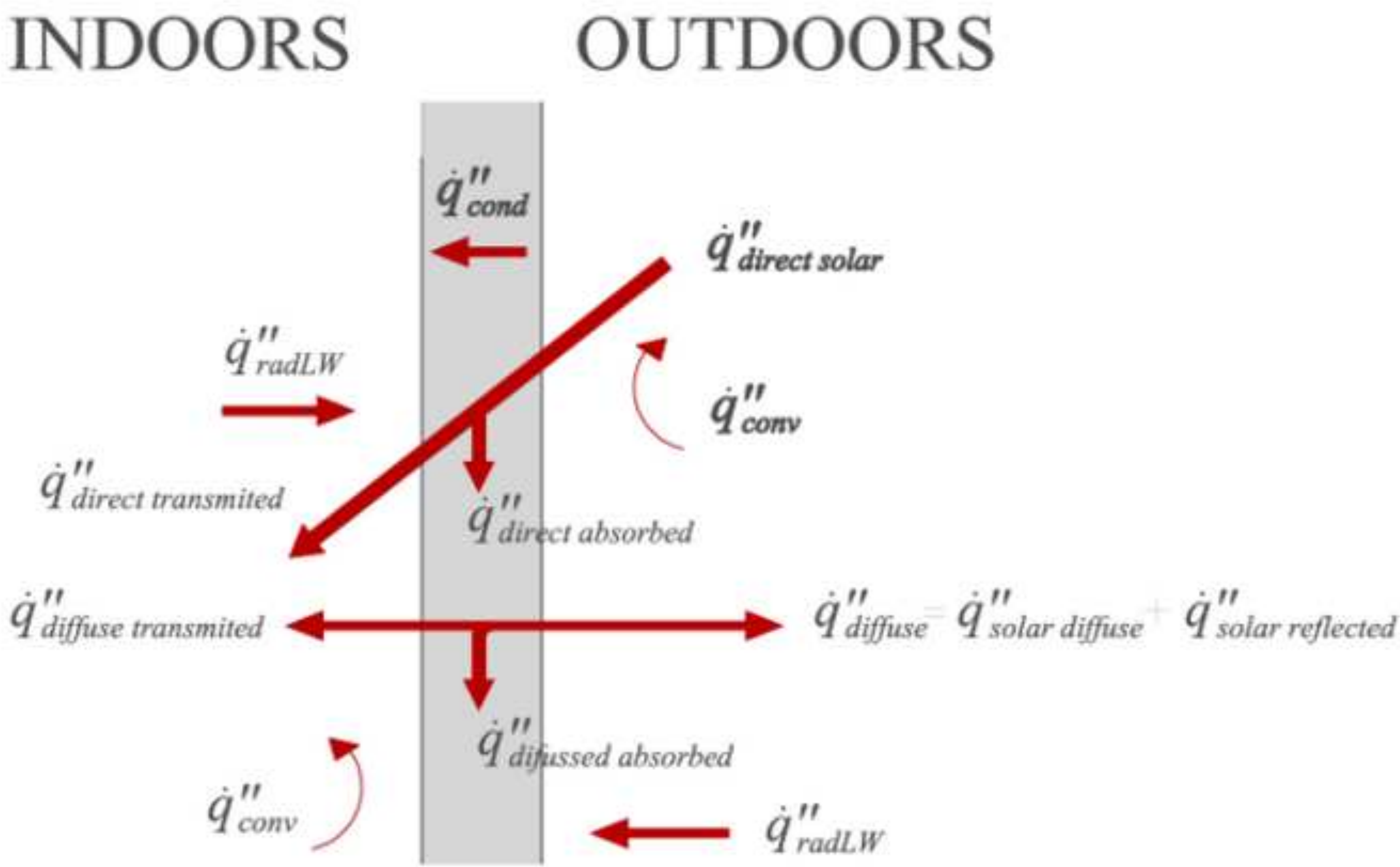

Figure(s)
Click here to download high resolution image

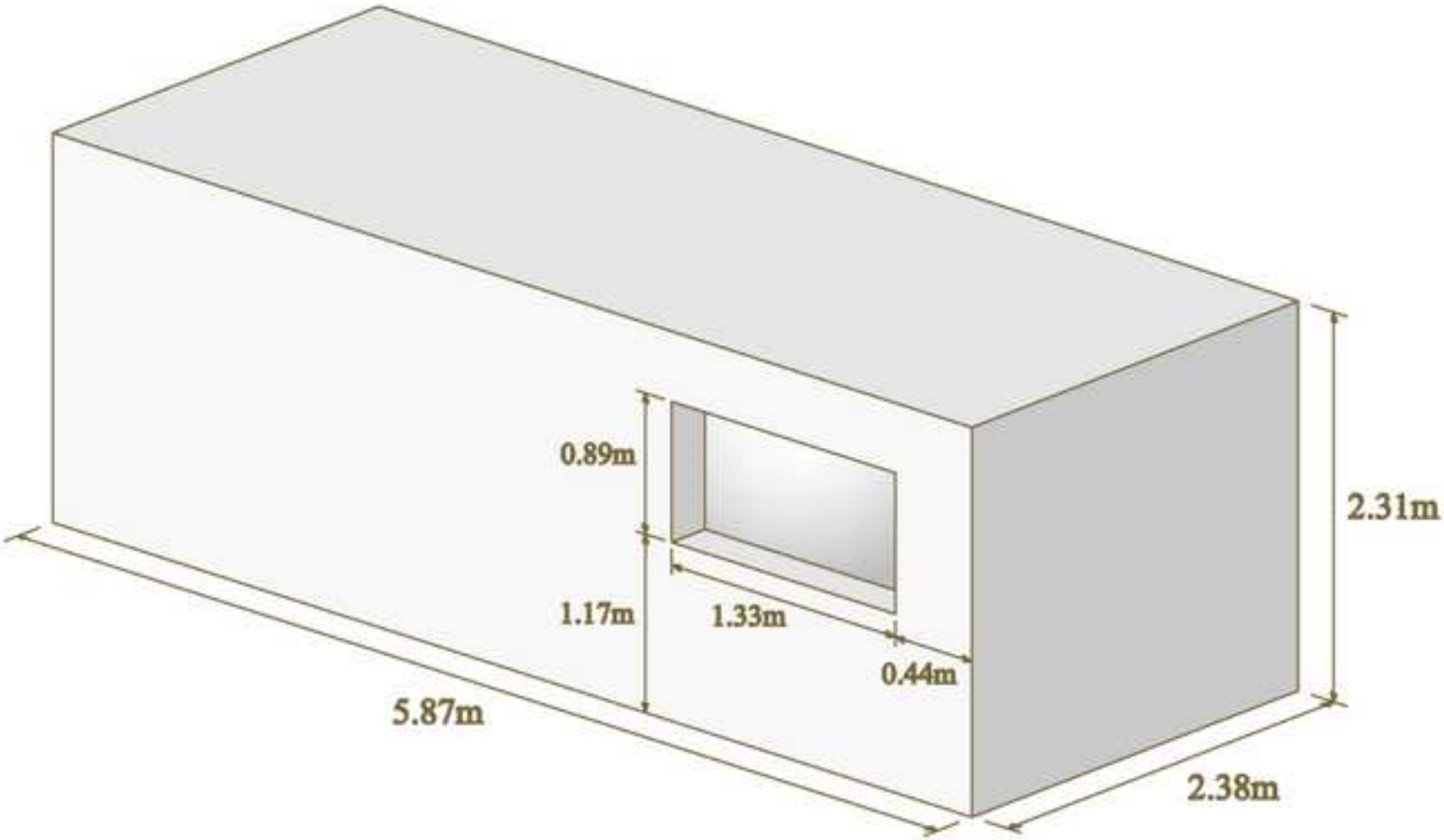

Figure(s)
Click here to download high resolution image

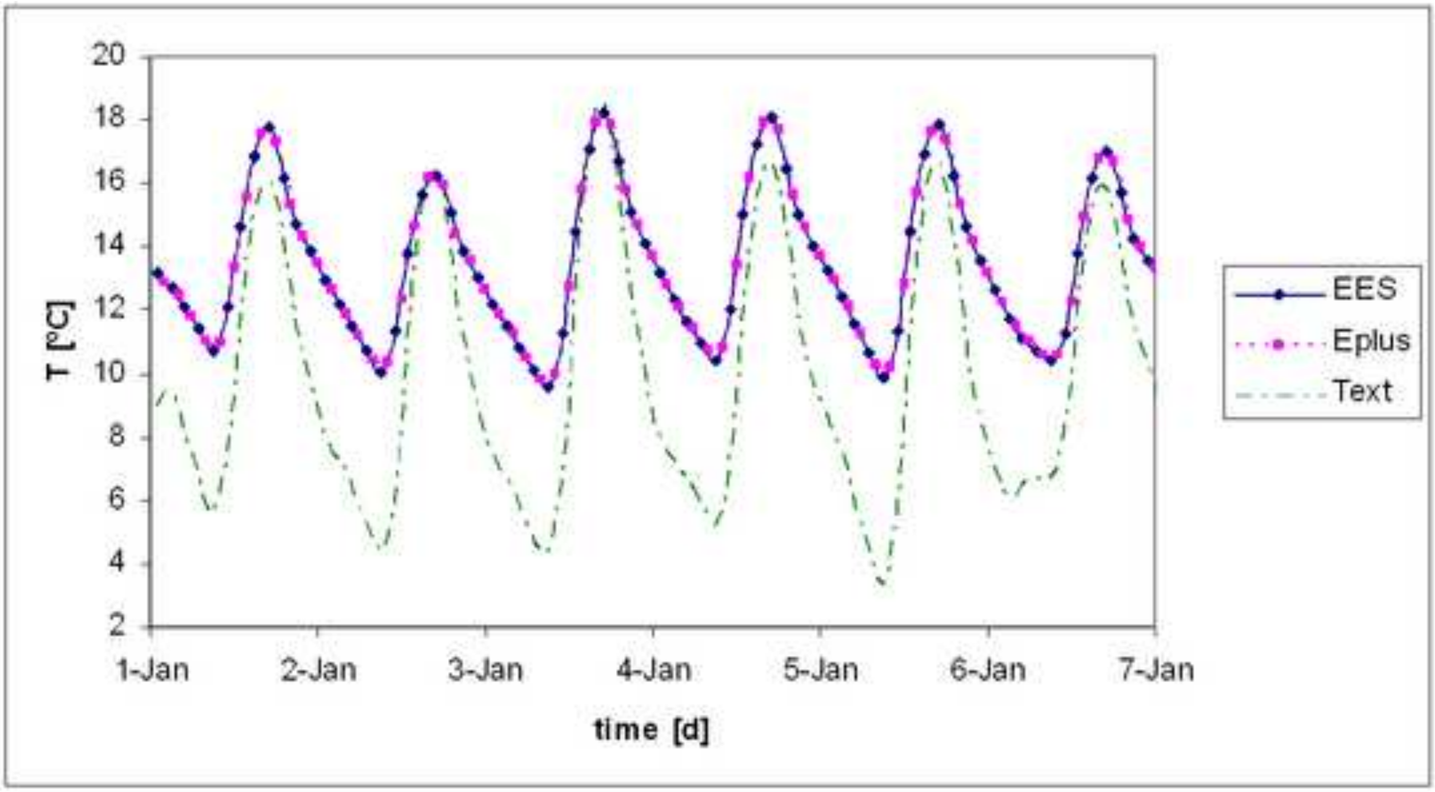

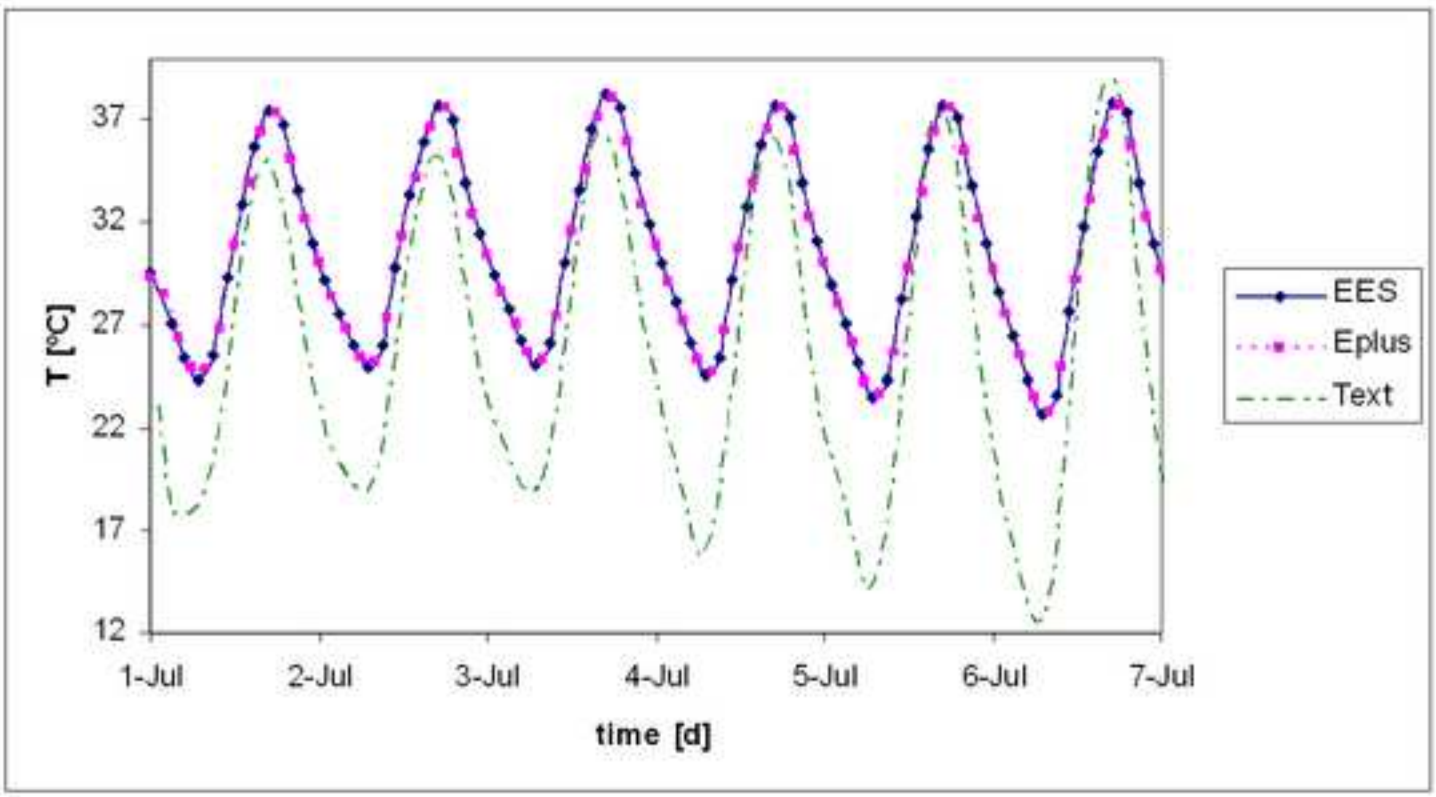

Figure(s)
Click here to download high resolution image

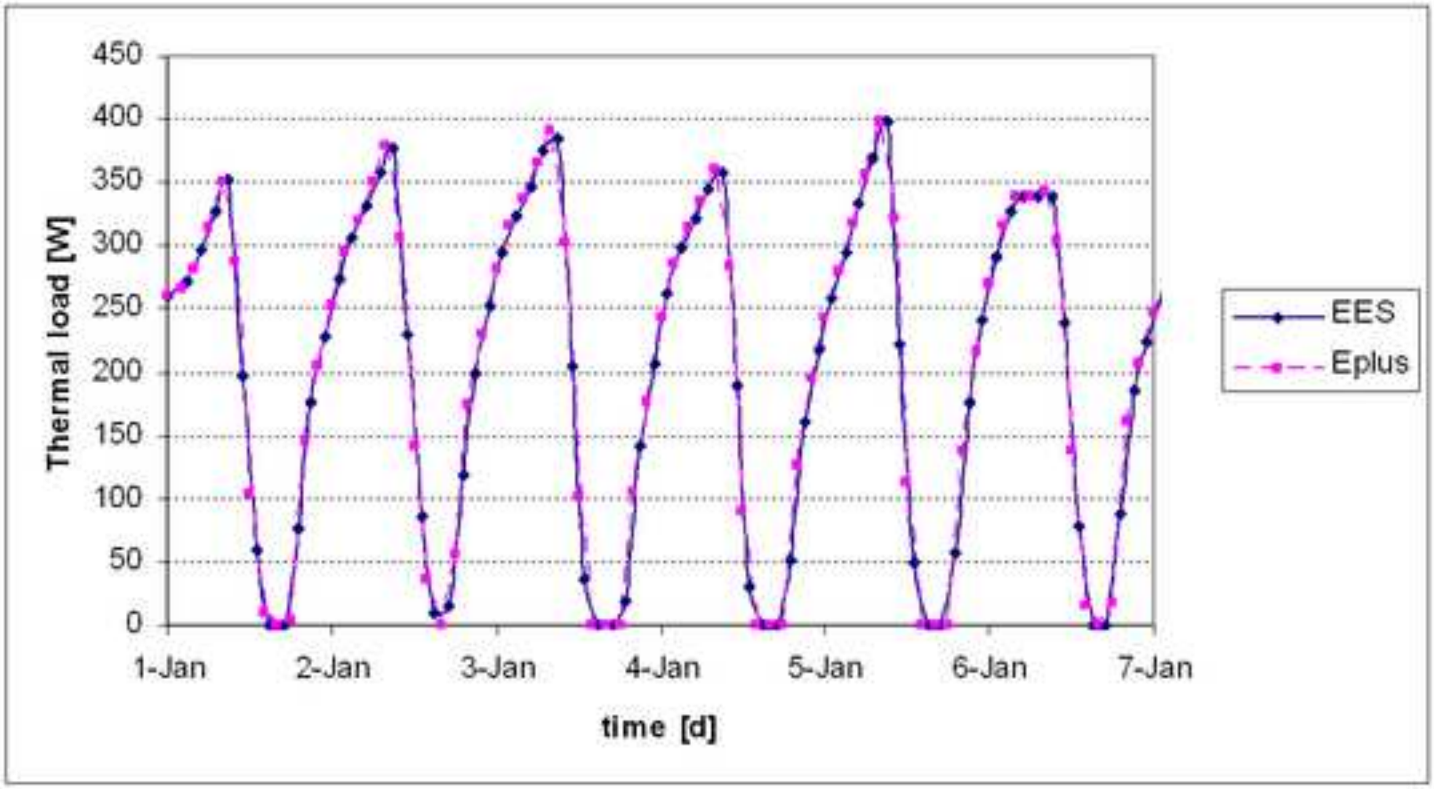

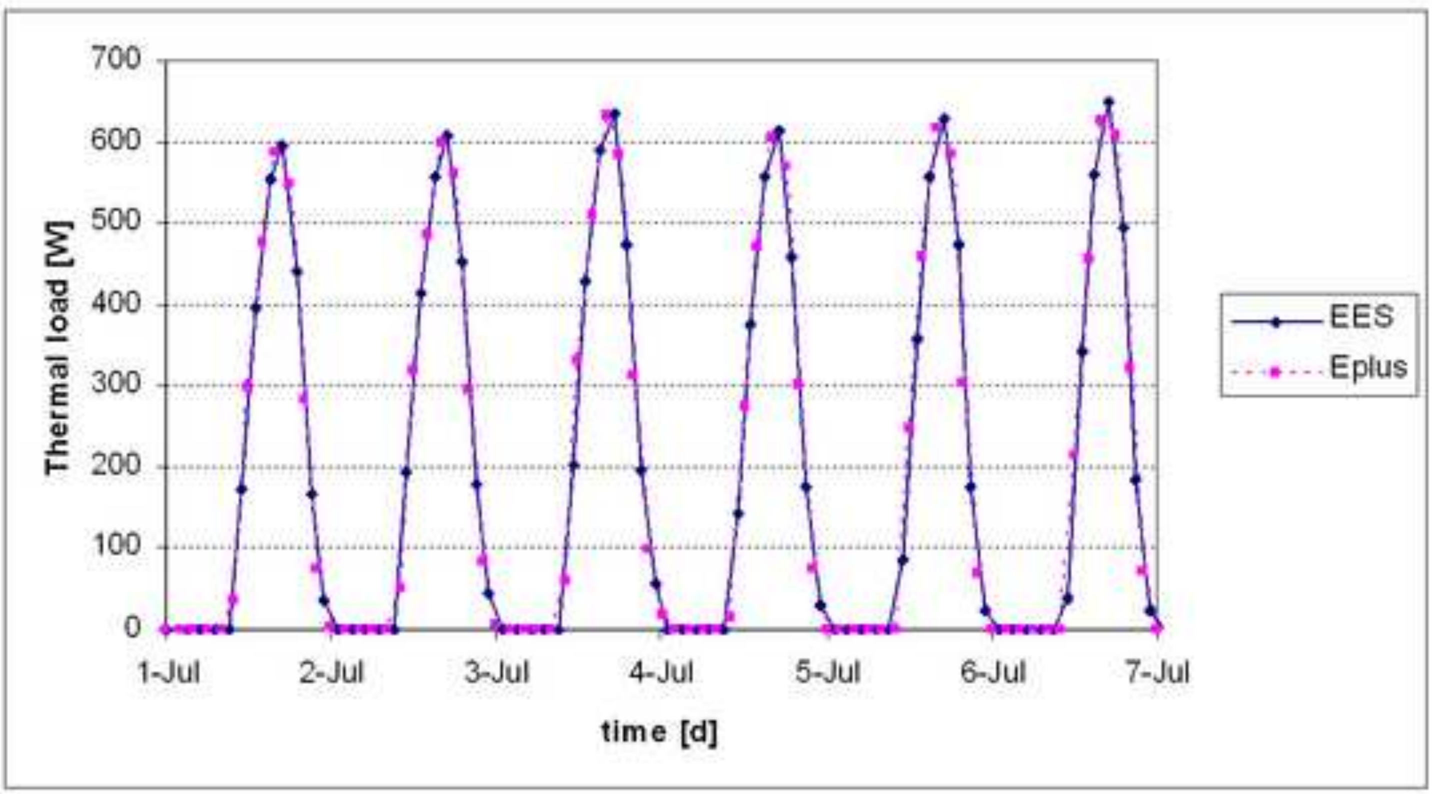

Figure(s)
Click here to download high resolution image

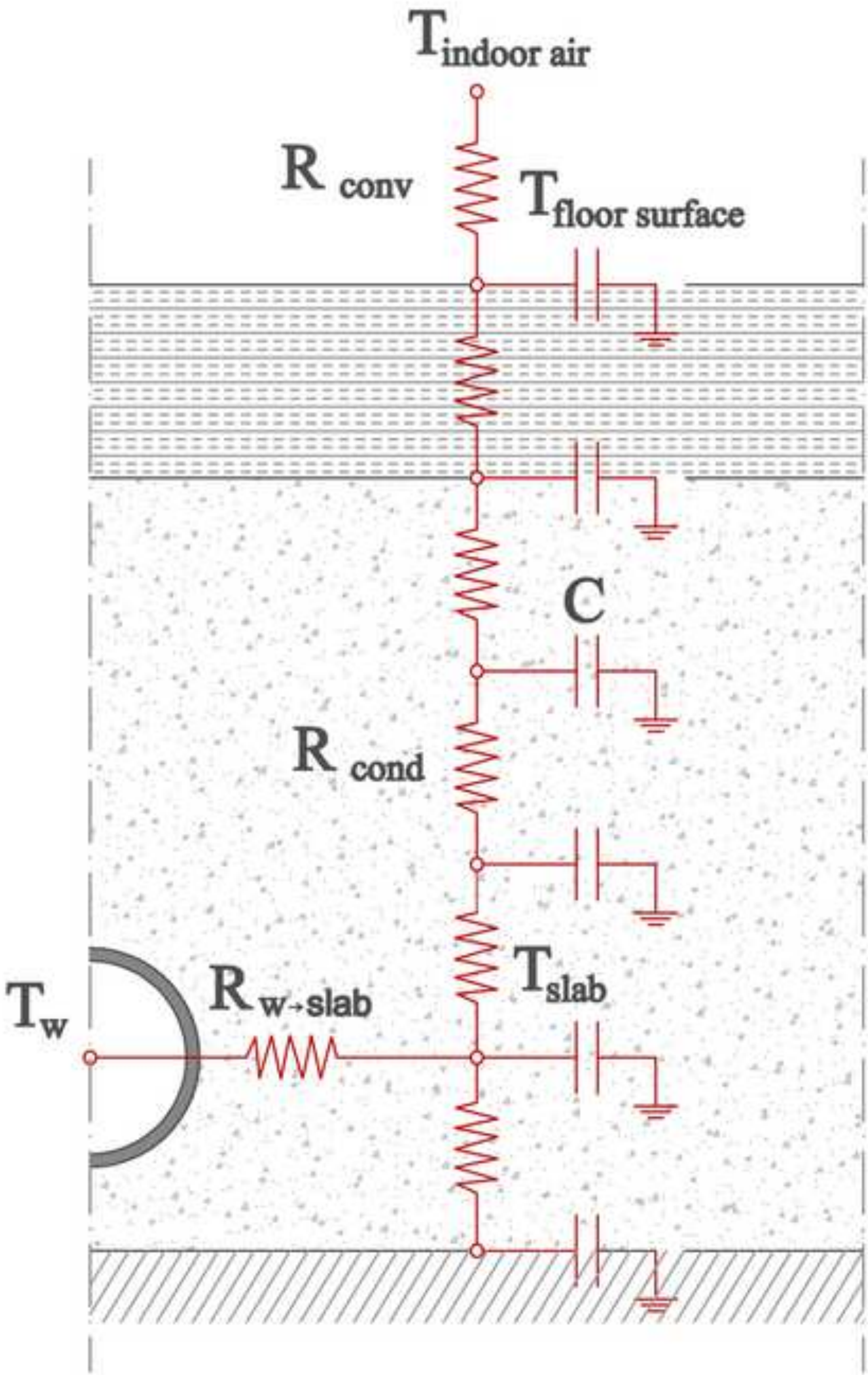

Figure(s)
Click here to download high resolution image

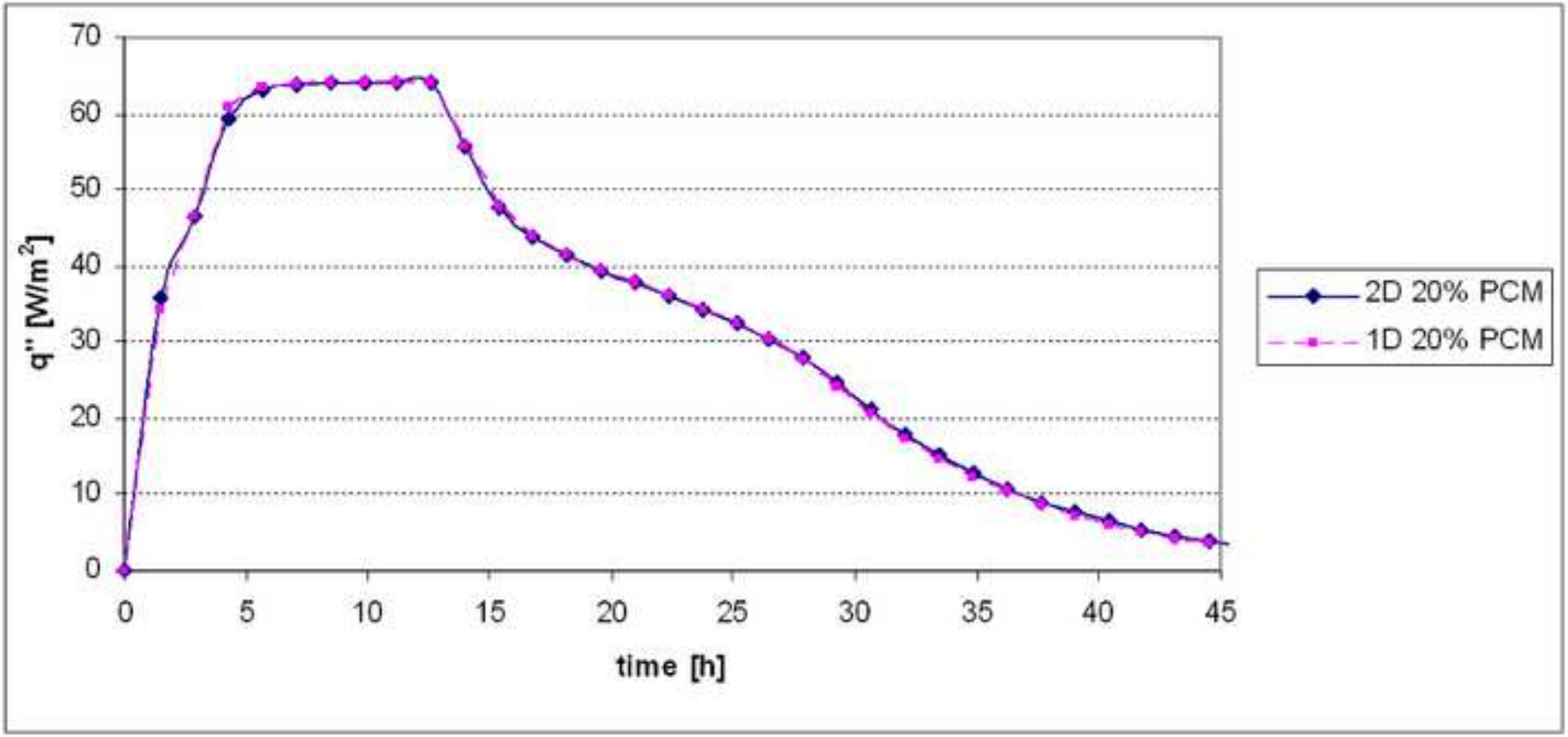

Figure(s)

Click here to download high resolution image

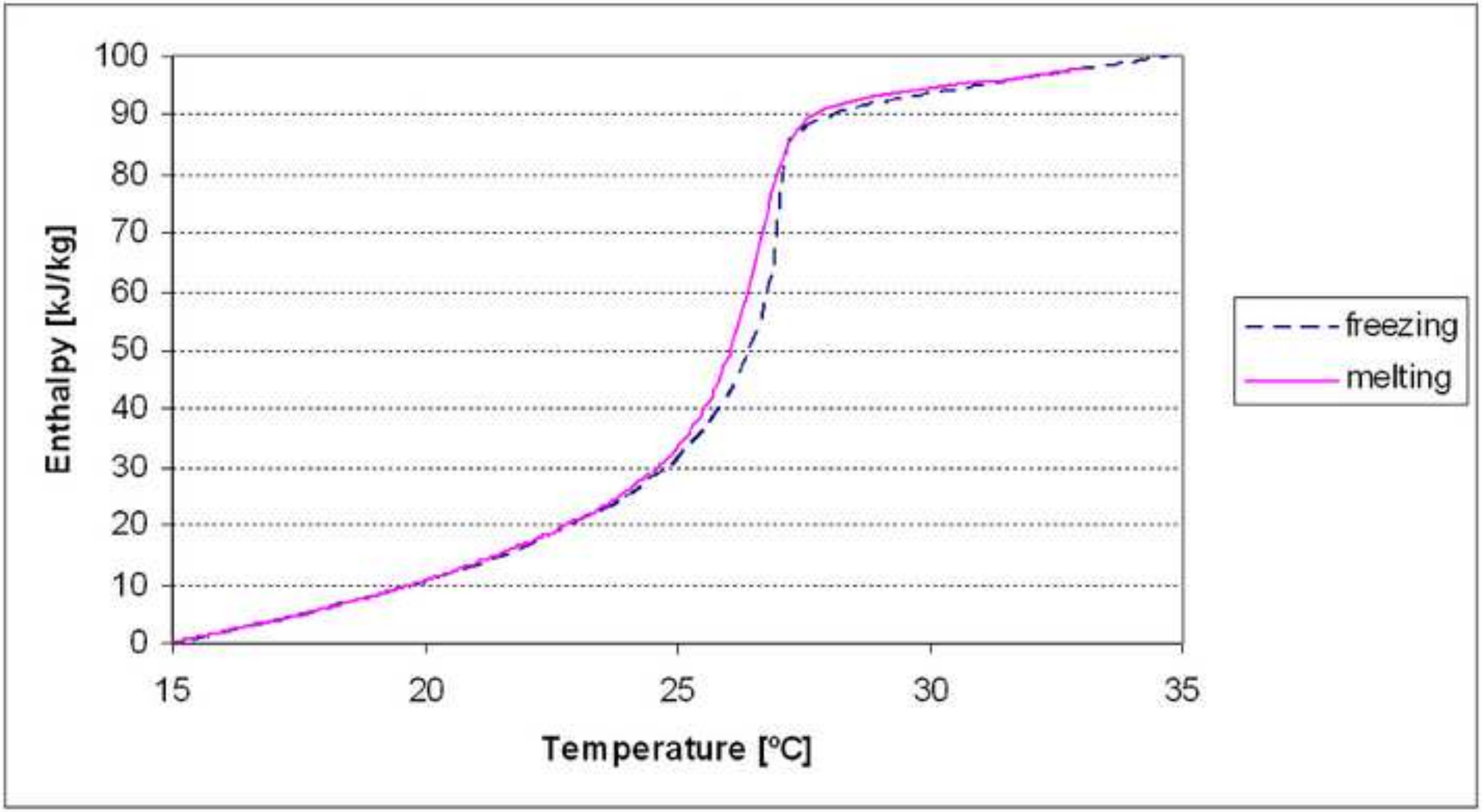

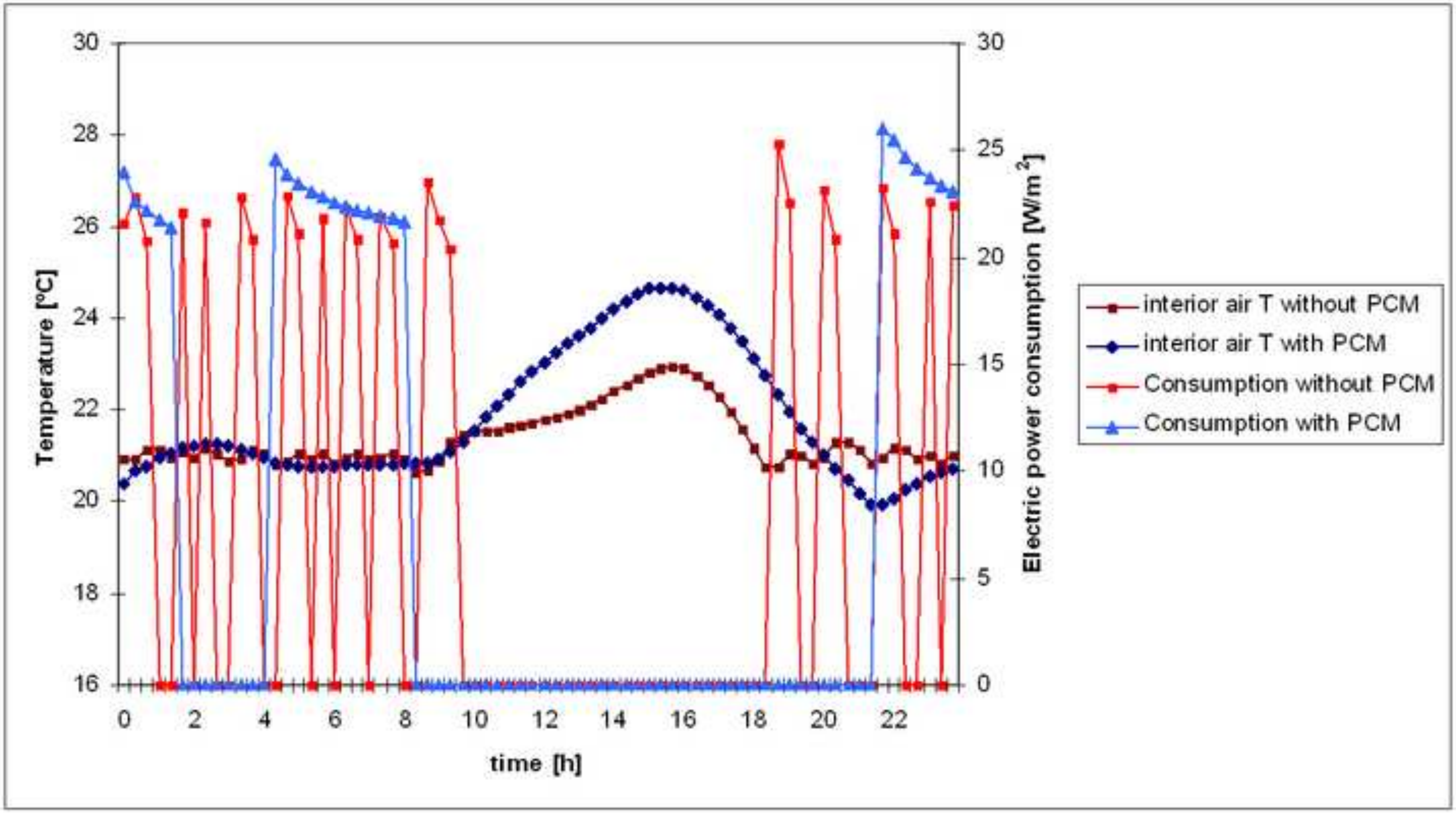
30
28
26
24
22
20
18
16
Temperature [ºC]
0
2
4
6
8
10
12
14
16
18
20
22
time [h]
30
25
20
15
10
5
0
Electric power consumption [W/m^2]
interior air T without PCM
interior air T with PCM
Consumption without PCM
Consumption with PCM

Figure(s)
Click here to download high resolution image

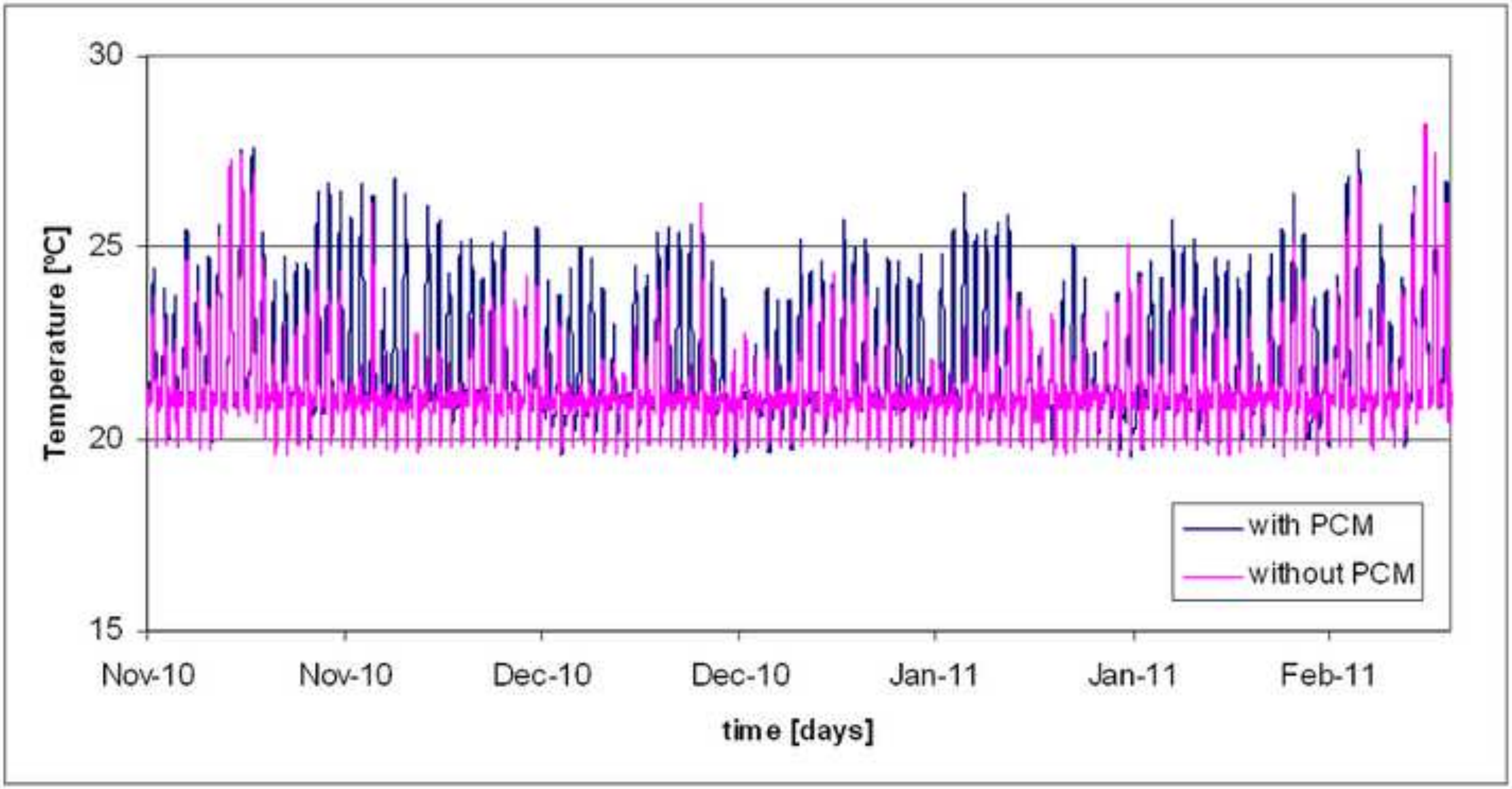

*Highlights

Highlights:

-A building simulation model has been developed to simulate a radiant floor with PCM.

-The building simulation model has been validated using Energy Plus.

-The behaviour of a PCM radiant floor system coupled to a heat pump has been analyzed.

-The PCM enables the shift of electric energy consumption to off-peak hours.